ARTICLES

Real-Time Propagation of the Reduced One-Electron Density Matrix in Atom-Centered Orbitals: Application to Multielectron Dynamics of Carbon Clusters C_n in the Strong Laser Pulses

Jin Sun, Jie Liu, and WanZhen Liang*

Hefei National Laboratory for Physical Science at Microscale, and Department of Chemical Physics, University of Science and Technology of China, Hefei 230026, P. R. China

Yi Zhao*

State Key Laboratory of Physical Chemistry of Solid Surfaces, and Department of Chemistry, Xiamen University, Xiamen, 361005, P. R. China

Received: May 19, 2008; Revised Manuscript Received: August 20, 2008

We present a time-dependent density functional theory (TDDFT) study on the electron dynamics of small carbon clusters C_n ($n = 9, 10$) exposed to a linearly polarized (LP) or circularly polarized (CP) oscillating electric field of ultrafast laser with moderate laser intensity. The multielectron dynamics is described by propagating the reduced one-electron density matrix in real-time domain. The high harmonic generation (HHG) spectra of emission as well as the time evolution of atomic charges, dipole moments and dipole accelerations during harmonic generation are calculated. The microscopic structure−property correlation of carbon chains is characterized. It is found that the electron responses of C_n to the laser field oscillation become nonadiabatic as the field intensity is larger than 1.4×10^{13} W/cm^2. The nonadiabatic multielectron effect is displayed by an explicit fluctuation on the induced atomic charges and the instantaneous dipole acceleration and by observing the additional peaks other than those predicted from the spectral selection rule in HHG spectra of C_n as well. The origin of these additional peaks is elucidated. The atomic charges of C_n in LP and CP laser pulses experience different type of oscillations as expected. In the linear structure C_9, the atomic charges at the two ends experience larger amplitude oscillations than those near the chain center whereas the induced charges on each atom of C_{10} experience the equal amplitude oscillations in the CP laser pulse.

1. Introduction

The natural time scale of electrons falls into the subfemtosecond or attosecond regime, which is much shorter than the vibrational periods of atoms in molecules. Therefore, the progress of laser technology capable of reaching subfemtosecond or attosecond pulse durations has enabled us to capture and steer the electron motion inside atoms and molecules that are undergoing photoionization or chemical change. Currently a new field called attosecond science, which probes the dynamical behavior of matter on the attosecond time scale, has thus formed. The recent advances in the attosecond science have been reviewed by a few groups.[1–6]

The quest to probe atomic and molecular electron dynamics on ultrashort timescales inevitably leads to the use of extreme ultraviolet (XUV)/X-ray radiation. High-harmonic generation (HHG) and stimulated Raman scattering, which generate frequency components over a wide range,[7] are two techniques to produce attosecond light pulses. The HHG process, in which visible or infrared laser light is converted to vacuum ultraviolet radiation, was known nearly two decades ago.[8] High harmonics from atoms have been extensively studied. An elegant and simple three-step quasi-static model, (1) tunnel ionization by an intense low-frequency laser field, (2) acceleration of the free electron, and (3) recollision, has successfully interpreted atomic HHG.[9] However, it is still a challenge to explain the high harmonics generated from polyatomic molecules because the electron dynamics of molecules is more complicated than that in isolated atoms due to the multiple nuclei and their relative motions.[10] Besides, molecular harmonics are very sensitive to the molecular orientation, the spatial arrangement of atoms in the molecule, and dynamic motion of the electrons.[11,12] The experiments on HHG of polyatomic molecules are thus far sparse. A few of theoretical works have investigated the mechanism of HHG from polyatomic molecules using a variety of theoretical approaches. For example, Zhang[13] calculated HHG of the C_{60} molecule using the time-dependent Hartree−Fock (TDHF) theory with a semiempiricial Hamiltonian and concluded that HHG are mainly from the multiple excitations and are intrinsic to the system. Averbukh et al.[14] showed that molecular HHG by CP laser field is a result of "bound-bound" transitions rather than "bound-continuum″ transitions, which dominate in the Corkum−Kulander recollision mechanism for atoms in a LP field. A more careful investigation on benzene has been performed by Baer et al.[15a] with respect to time-dependent density functional theory (TDDFT) with the adiabatic

* Corresponding authors. E-mail: liangwz@ustc.edu.cn (W.L.); yizhao@xmu.edu.cn.

10.1021/jp804408a CCC: $40.75
Published on Web 09/27/2008

local-density approximation. They found that for very strong fields (maximal strength larger than 3.5×10^{14} W/cm^2) ionization ceases well before the pulse reaches maximum and the recollision event is not observed, while for the pulse with the moderate laser intensity (maximal strength smaller than 1×10^{14} W/cm^2) the ionization continues throughout and the recollision event is observed. Therefore, the conjecture of Averbukh et al.[14] is that the dominant contribution to molecular HHG comes from the bound-bound transitions by using their model and that can only apply for stronger fields, above 1×10^{14} W/cm^2.

The goal of our work is to apply the TDDFT scheme to study the time-resolved electron dynamics of bare carbon chain systems driven by ultrashort laser pulses. TDDFT or TDHF theory, in its full extent without linear restrictions, can be applied directly to monitor the laser-driven electronic motion of multiphoton excitation with arbitrary laser pulse shape and duration. They, therefore, have been extensively used to study the intense field processes recently[13,15–24] although TDDFT with the adiabatic local-density approximation (LDA) may not be fully suitable for the strong field process.[25]

In the past decade, carbon chains of increasing complexity have been investigated by using a variety of spectroscopic techniques. One incentive for studying their electronic spectra has been their relevance to astrophysical observations, specifically, the absorptions toward reddened stars, discovered approximately one century ago through diffuse interstellar clouds.[26,27] The recent advances in the spectroscopy of carbon chains have been reviewed by Maier's group.[26] To date, no studies on the time-resolved electron dynamics driven by intense ultrashort laser pulses are found to the best of our knowledge. It is therefore interesting and meaningful for us to perform some studies on the laser-driven electron dynamics of C_n. Another motivation of our work to perform study on bare carbon chain systems C_n is due to their abundant conformations. Linear structures are stable for the small neutral carbon clusters with the cumulenic configurations (:C═C···C═C:), and the even-numbered species, C_4, C_6, C_8, and C_{10}, are recognized to have cyclic structures of comparable or even greater stability compared to the linear species.[28] Possibly different spatial arrangement of atoms in C_n provides us a chance to study how much the strong field response of a given molecule depends on the important properties such as molecular geometry and bonding.

To characterize the microscopic structure−property correlation of carbon chains, we calculate harmonic spectra generated by C_n in LP and CP fields and the time evolution of atomic charges, instantaneous dipole moments and dipole acceleration as well. The effects of molecular conformations, field intensities and field polarizations on HHG spectra and electron population are analyzed. In our simulations, Gaussian-type atomic orbital basis sets or the effective core potential (ECP) with its matching basis sets for valence electrons are used. This type of atom-centered localized orbitals may be inadequate to describe large amplitude motion of electrons. Thus, our simulations are in the case where no significant ionization is allowed. We avoid strong multiple ionization and subsequent Coulomb expansion by limiting the field intensity $I < 10^{14}$ W/cm ^{2} and the Keldysh parameter $\gamma \sim 1$. The Keldysh parameter,[29] defined as $\gamma = \omega_0[(2I_p)^{1/2}/E_{max}]$, provides a scalable gauge of the interaction dynamics and defines the limits between tunnel ($\gamma < 0.5$) and multiphoton ($\gamma \gg 1$) ionization. Here I_p is the ionization potential, E_{max} and ω_0 are the amplitude and frequency of the laser field, respectively. The atomic units are used throughout the paper. The range of intermediate $\gamma \sim 1$, which is typical for most current intense field experiments, is the regime of nonadiabatic tunnelling. At this regime, the popular quasi-static tunnel models of strong field molecular ionization, based upon the adiabatic response of a single active electron, may be inadequate for a molecule with delocalized electrons.

The paper is organized as follows. In section 2, we summarize the TDDFT scheme using the density matrix and atom-centered basis functions. In section 3, the electronic properties of small carbon clusters C_n, such as harmonics and the laser-induced atomic charges are calculated and reported. The laser parameters, i.e., the external field polarizations, frequencies, and intensities are varied to check how HHG and atomic charges change accordingly. Finally, conclusions are given in section 4.

2. Computational Method

HHG can be viewed as the power radiated by a system in the strong field, which depends on the acceleration of atomic electron.[30] It is proportional to the square of Fourier transform of the time-dependent dipole acceleration, which is defined as

$$\ddot{d}(t) = \frac{d^2\langle\Psi(r,t)|\hat{\mu}|\Psi(r,t)\rangle}{dt^2} \quad (1)$$

where $\hat{\mu}$ is the molecular dipolar operator and $\Psi(t)$ is the time-dependent wave function which can be obtained by solving the time-dependent Schrödinger equation directly in real-time and real-space. With the one-electron reduced density matrix ρ, the dipole acceleration can be alternatively written as

$$\ddot{d}(t) = \frac{d^2}{dt^2} Tr(\rho(t)\mu) \quad (2)$$

The finite difference method is used to calculate $\ddot{d}(t)$ in this work. The density matrix version of TDHF/TDDFT equation with the generalized nonorthogonal basis sets can be expressed as[31]

$$i\hbar S\frac{d\rho^{\sigma}_{AO}(t)}{dt}S = F^{\sigma}_{AO}(t)\rho^{\sigma}_{AO}(t)S - S\rho^{\sigma}_{AO}(t)F^{\sigma}_{AO}(t) \quad (3)$$

where F^{σ}_{AO} denotes the one-body effective Hamiltonian. It relates to the density as follows:

$$F^{\sigma}_{AO}(r) = -\frac{1}{2}\nabla^2 + V_{ext}(r) + \int\frac{\rho_{AO}(r')}{|r-r'|}dr' + V^{\sigma}_{xc}(r) \quad (4)$$

$V^{\sigma}_{xc}(r)$ is the exchange-correlation potential. In eq 3, the AO basis overlap matrix S comes from the nonorthogonal basis set. Utilizing Löwdin orthogonalization procedure, i.e., $F = S^{-1/2} F_{AO} S^{-1/2}$ and $\rho = S^{1/2}\ \rho_{AO} S^{1/2}$, the TDDFT equation in the nonorthogonalized basis set can be casted into

$$i\hbar\frac{d\rho^{\sigma}(t)}{dt} = F^{\sigma}(t)\rho^{\sigma}(t) - \rho^{\sigma}(t)F^{\sigma}(t) \quad (5)$$

Numerically, we employ the second-order Magnus integration method with the matrix polynomial expansion of the evolution operator to solve eq 5. The detailed description has been given in ref 32. With obtained $\rho(t)$, we calculate $d(t) = Tr(\rho(t)\mu)$, and the finite difference method is adopted in the calculation of $\ddot{d}(t)$.

In the present work, we investigate the interaction of both the LP and CP laser pulses with linear and cyclic structure carbon clusters. The polarized laser pulse is specified by $E(t) = E_{max}\, s(t)(\cos(\omega t)\hat{\imath} + \lambda \sin(\omega t)\hat{\jmath})$ with the pulse shape function $s(t) = \sin^2(\pi t/t_p)$. Here t_p denotes the total duration of the laser pulse. $\lambda = 0$ is for the LP laser pulse and $\lambda = \pm 1$ for the left/

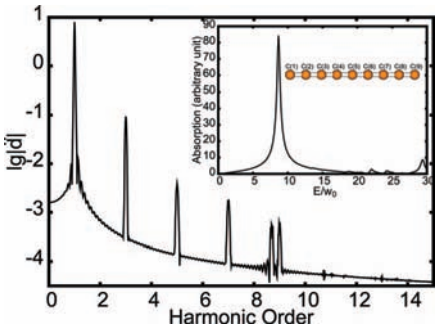

Figure 1. Harmonics generated by C_9 in LP field with $\omega_0 = 0.02$, $E_{max} = 0.02$, and the pulse duration $t_p = 50\tau$ ($\tau = 2\pi/\omega_0$). The inset is the absorption spectrum. For comparison, the absorption energy is scaled by a factor of $1/\omega_0$. Except the results in Figure 2, all other results are produced by using the ECP CRENBL with its matching orbital basis set for the valence electrons.

right CP laser pulses. The polarization direction of LP laser field is set along the long chain and that of CP laser field is set to be perpendicular to the N-fold rotational symmetry axis of cyclic structure C_{2N}.

3. Results and Discussions

We implemented the TDDFT scheme in the development version of the Q-Chem software package.[33] The hybrid exchange-correlation functional B3LYP[34] and the effective core potential (ECP) CRENBL[35] are applied. In Q-Chem, each of the built-in ECPs comes with a matching orbital basis set for the valence electrons. B3LYP partially includes the exact HF exchange term and may partially overcome the self-interaction error while LDA suffers a severe deficiency, namely, the corresponding xc potentials do not possess the correct long-range behavior which may lead to the ionization potentials and the excited-state energies to be 30−40% low.[23,36] The reduced one-electron density matrix is propagated with a time step-size of 0.2 au (1 fs = 41.34 atomic unit time). The molecular equilibrium geometries and the electronic structures in the ground-state are taken as the initial condition. The phase of the laser field is chosen to be zero and the nuclei are not permitted to move.

3.1. Harmonics Generated by the Cyclic Structure C_{10} and Linear Chain C_9. Figures 1−3 show the calculated harmonics spectra generated by the linear chain C_9 and cyclic structure C_{10}, respectively. When C_9 and C_{10} are exposed to a LP laser field directed along the long chain, without exception, we only observe the odd-order harmonics due to the inversion symmetry of molecules. A relatively weak laser pulse can generate efficient HHG for carbon chains. The maximal harmonic orders can be extended to 10th in C_9 even if the laser intensity is weak to 1.4×10^{13} W/cm ^{2} ($|E_{max}| = 0.02$ au).

Unlike harmonic spectra in LP laser field, harmonics generated by C_{10} in CP laser field show quite different spectral characters (see Figures 2 and 3). They include both odd- and even-order harmonics. For instance, 4th, 6th, 9th, 11th,..., order harmonics are observed. The dynamical symmetry of the time periodic Hamiltonian combined with Floquet formalism has been applied to predict which order of harmonics are allowed in the cyclic molecules.[37] The approach assumed that the system driven by a periodically time-dependent field is in a pure field-dressed Floquet state. Therefore, the probability of getting the nth harmonic in a Floquet state $\Psi_W(\vec{r}, t)$ of a system ($\Psi_W(\vec{r}, t) = \Phi(\vec{r}, t)e^{-iWt}$, where W is the quasi-energy, $\Phi(\vec{r}, t + \tau) = \Phi(\vec{r}, t)$, and $\tau = 2\hbar\pi/\omega$) can be written as

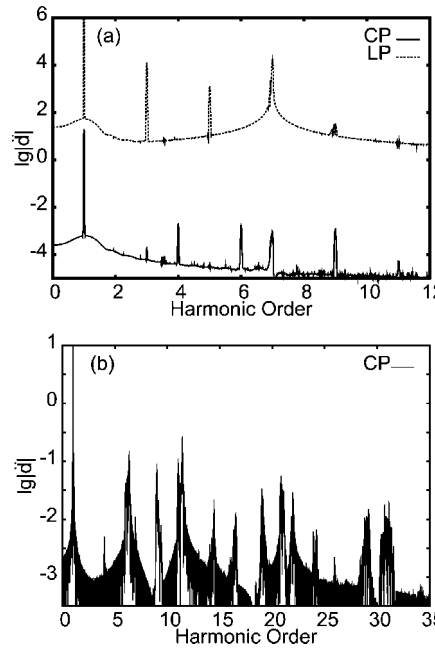

Figure 2. (a) Harmonics generated by C_{10} in LP and CP fields with $\omega_0 = 0.04$, $E_{max} = 0.03$, and $t_p = 120\tau$. The overall harmonic spectrum of C_{10} in LP laser field is upwardly shifted by 4. (b) Harmonics generated by C_{10} in CP field with $\omega_0 = 0.04$, $E_{max} = 0.05$, and $t_p = 50\tau$. The Pople full-electron basis 6-31G** is applied to produce the results in this figure.

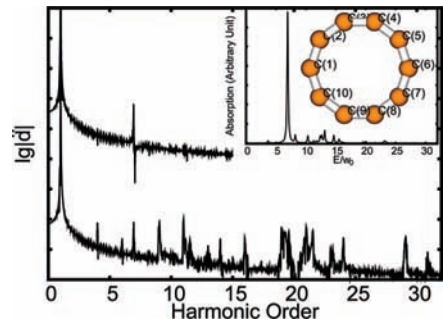

Figure 3. Harmonics generated by C_{10} in CP field with $\omega_0 = 0.04$ and $t_p = 50\tau$. The field amplitude is changed from $E_{max} = 0.01$ to 0.02. The inset is the absorption spectrum.

$$\sigma_W^n \propto n^4 |\langle\langle \Phi(\vec{r}, t)|\hat{\mu}e^{-in\omega t}|\Phi(\vec{r}, t)\rangle\rangle|^2 \qquad (6)$$

where the double braket notation, $\langle\langle \cdots \rangle\rangle$ stands for the integration over spatial variables and time. When the Hamiltonian $H(t) = H(t) - i\partial/\partial t$ is invariant under dynamical symmetry of order N, ref 37 derived the HHG spectral selection rule, the nth order harmonic emits only when n satisfies the condition $n = kN \pm 1$. Therefore, the higher the symmetry order N, the less the generated harmonics within a fixed frequency interval.

The point group of C_{10} belongs to D_{5h}. When it interacts with a CP laser pulse with sufficiently long duration, its molecular Hamiltonian has the symmetry group G_5. Therefore, one can derive the spectral SR: $n = 5k \pm 1$ for C_{10} with respect to the Floquet formalism. However, the system may not be in a pure field-dressed Floquet state for the subfemtosecond laser pulse. This may result in additional peaks other than those predicted from the spectral selection rule to be present.[38,39] For instance, the peak near the 7th order appears in HHG spectra of C_{10} in both LP and CP field (see Figure 2) and the peak near 9th order is observed in HHG spectra of C_9 in LP field.

To identify the origin of these additional peaks, we calculate the absorption spectra of C_9 and C_{10} in a relatively weak field

(E_{max} = 0.001 au). Comparing the HHG spectra with the absorption spectra, we observe that the additional peaks prefer to being generated near the positions with the excitation energies corresponding to the strongest absorption peaks. For example, the absorption peak with the excitation energy Δ = 7.56 eV and the transition dipole moment $|\mu|$ = 3.35 au for C_{10} and that with Δ = 4.7 eV and $|\mu|$ = 6.4 au for C_9. Lezius et al. in ref 40 called the excited-state which is most strongly coupled to the ground-state as the doorway state. Through it, electrons are excited to a quasicontinuum (QC) of excited-states. The QC is formed as the intense laser field shifts and mixes the energy levels of the excited-state manifold, thus allowing electrons to rapidly climb up and ionize. When the electron response to the laser field oscillation becomes nonadiabatic, Landau−Zener type nonadiabatic transitions become increasingly probable, allowing population to evolve toward higher-lying (bound) electronic states. At $\omega_0 E_{max} L \sim \Delta$,[2] this nonadiabatic transition which corresponds to charge transfer across the molecule is quickly saturated, leading to strong nonresonant absorption by all delocalized electrons involved in this coupling,[40] where L is the characteristic length of system.

The electrons which transit to the doorway state via the nonresonant absorption may quickly back to the ground-state by emitting a radiation or rapidly climb up to QC and ionize. It is apparent that the peaks near 9th order in HHG of C_9 and 7th order in HHG of C_{10} originate from the population of the doorway states. Because of fast saturation of the nonadiabatic transition, in this limit, nonresonant energy absorption becomes only weakly sensitive to laser intensity. This explains the reason why the relatively intensities of these additional peaks reduce (see the peak near 7th order in Figure 2) as the field intensity increases. They may not be observed in the HHG spectra when one further increases the intensity of laser pulses. The ionization probabilities may be predicted by the nonadiabatic multielectron (NME) theory.[40] The Landau−Zener-type nonadiabatic transition probability, defined as $P_{LZ} \sim \exp(-\pi\Delta^2/(4\omega_0 E_{max} L))$, respectively predicts an maximum ionization probability 2×10^{-5} and 1.7×10^{-3} for C_{10} at ω_0 = 0.04 au, E_{max} = 0.03 and 0.05 au during one-half a laser cycle, where L is set to $\sqrt{2.0}\,\mu$ by considering the effect of LP pulses. It is apparent that, under the conditions of our simulations, NME predicts no significant ionization.

As E_{max} increases to 0.05 au, more higher-lying excited states can be populated and the ionization probability increases. More electrons can be ionized. The ionized electrons recollide with the atomic nuclei and create additional emission channels even for molecular HHG in CP fields at this moderate laser intensity. The effect of basis set is checked. Figure 3 shows the harmonics generated by using ECP CRENBL with a matching orbital basis set for the valence electrons. Comparing HHG in Figures 2 and 3, the effect of basis set on electron spectra is significant. Even with a weaker field E_{max} = 0.02 au, the maximum order harmonic generated by using ECP is same with that using the Pople basis set 6-31G** at E_{max} = 0.05 au. Larger basis set including diffuse functions and continuum functions is expected to more exactly describe HHG of polyatomic molecules.

3.2. Instantaneous Electron Population Analysis. To obtain the detailed knowledge of the laser-driven electron dynamics, we display the time evolution of atomic charges. The data offer the underlying information about the evolution of the electron wave function during harmonic generation. The field-induced effective charge on the Nth carbon atom is defined as $P_N(t) = \Sigma_{p\in N}\delta\rho_{pp}(t)$. At time t, the total field-induced effective charge on molecule should be zero. The field-induced density matrix $\delta\rho(t) = \rho(t) - \rho(0)$ is obtained by solving eq 5 in real-time domain. In Figure 4, we plot the charge movement for the linear structure C_9 cluster in the LP laser pulse. Löwdin population analysis reveals that the predominant amount of charges induced by the field locate at two ends of C_9 with opposite charge values. It indicates that the induced charges at two sides experience larger amplitude oscillations than those near the chain center, and there is a phase difference π between the phases of oscillating charges of two atoms which are symmetrically located at two sides of the chain center in C_9. Figure 5 displays the charge movement for C_{10} in CP laser pulses. Unlike C_9 in the LP pulse, the induced charges on each atom of C_{10} oscillate in both x and y directions following the external fields. The oscillating amplitudes on x and y directions depend on the coordinates of C atoms. However, the total amplitude of the induced charges on each atom of C_{10} is same in CP pulses. One may expect to observe unidirectional valence-type electronic ring currents in C_{10} cluster driven by a ultrashort CP laser pulse within the pulse duration. The similar behavior has been observed by Barth et al. in the oriented molecule Mg−porphyrin excited by a ultrashort laser pulse.[41,42]

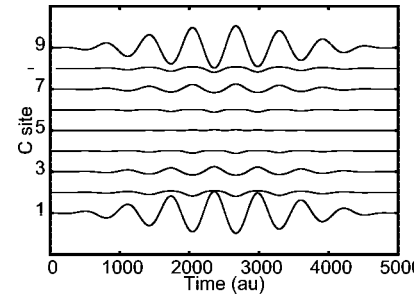

Figure 4. Field-induced atomic charges of C_9 in LP laser pulse with ω_0 = 0.01, E_{max} = 0.01, and $t_p = 8\tau$.

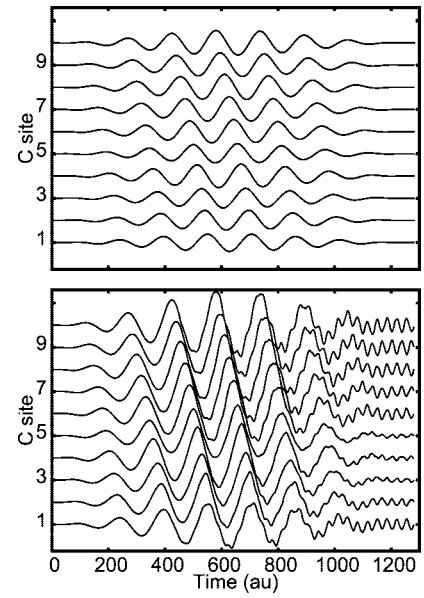

Figure 5. Field-induced atomic charges of C_{10} in CP laser pulses with ω_0 = 0.04, $t_p = 8\tau$, and varied E_{max}. E_{max} = 0.02 in the upper panel and E_{max} = 0.05 in the lower panel.

3.3. Nonadiabatic Effects of Electron Response to the Ultrafast Laser Pulses. To further understand the interaction between the external field and the system, we investigate the dependence of the instantaneous dipole $d(t)$ and dipole acceleration $\ddot{d}(t)$ of C_{10} on the intensities and frequencies of laser fields. It can be seen from Figure 5 that the electron response follows the external field adiabatically when a relatively weak field

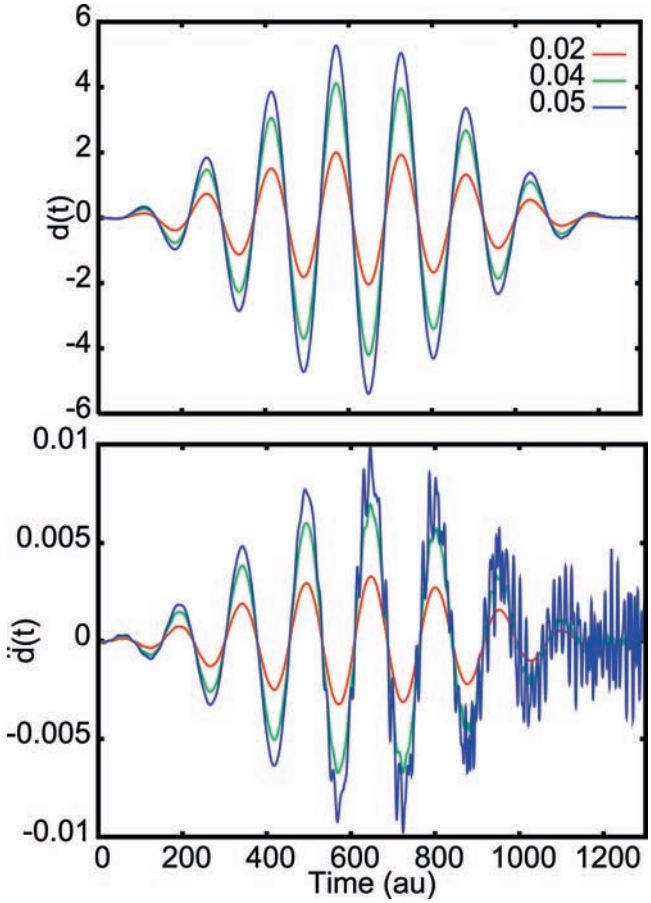

Figure 6. Field-induced dipole $d(t) = Tr(\delta\rho\mu)$ and dipole acceleration $S(t) = \ddot{d}(t)$ of C_{10} in CP laser field with $\omega_0 = 0.04$, $t_p = 8\tau$, and varied E_{max}. Red line: $E_{max} = 0.02$; green line: $E_{max} = 0.04$; blue line $E_{max} = 0.05$.

($E_{max} = 0.02$ au and $\omega_0 = 0.04$ au) is applied; that is, when the field strength passes through zero and after the field is turned off, the induced charge on each carbon atom is close to zero. Meanwhile, both $d(t)$ and $\ddot{d}(t)$ follow the field adiabatically, too. As E_{max} increases to 0.04 au, however, electron response of C_{10} to the external field is more complicated. An explicit fluctuation of the induced atomic charges caused by the oscillation of the molecular orbital populations are observed and when the field returns to zero, small oscillations of the charge continue. At this level, although $d(t)$ adjusts instantaneously to the time-varying electric field $E(t)$ of the laser, the nonadiabatic effect starts to show on $\ddot{d}(t)$ (see Figure 6). One observes small oscillations to be present on $\ddot{d}(t)$ after the 4th optical cycle of the field. In this case, a maximal field intensity of 5.62×10^{13} W/cm^2 ($|E_{max}| = 0.04$ au) yields a Keldysh parameter of $\gamma = 0.86$ (I_p of C_{10} is estimated to be ca. 10.0 eV[28]), indicating that the strong field ionization is near the tunnel ionization regime. At this regime, for the molecules with larger delocalized electron path length L, the nonadiabatic multielectron effect is still pronounced,[40] which gives rise to the higher-lying (bound) electronic states populated during the laser duration and results in small oscillations in $d(t)$ and $\ddot{d}(t)$. Furthermore, these higher-lying excited states remain populated after the pulse passes over. Therefore, $d(t)$ and $\ddot{d}(t)$ keep oscillations and do not return to zero when the field is turned off. The corresponding fluctuations in the instantaneous dipole acceleration are more drastic than in the dipole moment (see Figure 6).

Figure 7 displays the laser frequency dependence of the nonadiabatic effects. As expected, when the laser frequency is close to the resonant frequency of the molecule, more electrons are transited and the fluctuations in the instantaneous dipole acceleration become more pronounced.

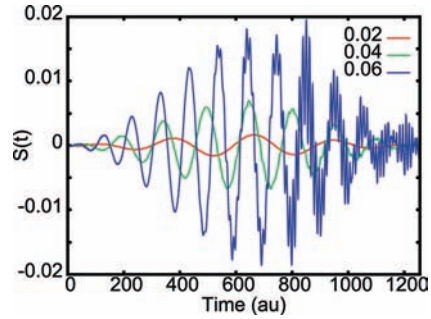

Figure 7. $\ddot{d}(t)$ of C_{10} in CP laser pulse with $E_{max} = 0.04$, $t_p = 1256$, and varied field frequencies ω_0. Red line: $\omega_0 = 0.02$; green line: $\omega_0 = 0.04$; blue line $\omega_0 = 0.06$.

4. Concluding Remarks

We have numerically investigated the electron dynamics of small carbon clusters in the short LP and CP laser fields systematically based on TDDFT. Both harmonic generation and laser-driven electron dynamics are studied and displayed. We find that electron response of small carbon clusters to the fields is complicated. When the field is weak, the electron response follows the external field adiabatically. When the electron response to the laser field oscillation becomes nonadiabatic, we observe the explicit fluctuations of atomic charges and the instantaneous dipole acceleration resulted from the population of the higher-lying (bound) electronic states during the laser duration. The superposition of excited states also result in the additional peaks other than the spectral selection rule to be present on HHG of small carbon clusters at the moderate laser intensity. The origination of additional peaks has been explained with respect to the nonadiabatic multielectron dynamics.

Acknowledgment. Financial support from National Science Foundation of China (Nos. 20673104 and 50121202) and a 973 project funded by National Basic Research Program of China (Nos. 2004CB719901 and 2007CB815204) are acknowledged.

References and Notes

(1) Bucksbaum, P. H. *Science* **2007**, *317*, 766.
(2) Goulielmkis, E.; Yakovlev, V. S.; Cavalieri, A. L.; Uiberacker, M.; Pervak, V.; Apolonski, A.; Kienberger, R.; Kleineberg, U.; Krausz, F. *Science* **2007**, *317*, 769.
(3) Kapteyn, H.; Cohen, O.; Christov, I.; Murnane, M. *Science* **2007**, *317*, 775.
(4) Calvayrac, F.; Reinhard, P. G.; Suraud, E.; Ullrich, C. A. *Phys. Reports* **2000**, *337*, 493.
(5) Kling, M. F.; Vrakking, M. J. J. *Annu. Rev. Phys. Chem.* **2008**, *59*, 463.
(6) Winterfeldt, C.; Spielmann, C.; Gerber, G. *Rev. Mod. Phys.* **2008**, *80*, 117.
(7) (a) Farkas, G.; Toth, C. *Phys. Lett. A* **1992**, *168*, 447. (b) Antoine, P.; L'Huillier, A.; Lewenstein, M. *Phys. Rev. Lett.* **1996**, *77*, 1234. (c) Antoine, P.; Milosevic, D. B.; L'Huillier, A.; Gaarde, M. B.; Salieres, P.; Lewenstein, M. *Phys. Rev. A* **1997**, *56*, 4960. (d) Harris, S. E.; Sokolov, A. V. *Phys. Rev. Lett.* **1998**, *81*, 2894.
(8) Ferray, M.; L'Huillier, A.; Li, X. F.; Lompre, L. A.; Mainfray, G.; Manus, C. *J. Phys. B* **1988**, *21*, L31.
(9) Corkum, P. B. *Phys. Rev. Lett.* **1993**, *71*, 1994.
(10) Hay, N.; Nalda, R. de; Halfmann, T.; Mendham, K. J; Mason, M. B.; Castillejo, M.; Marangos, J. P. *Eur. Phys. J. D* **2001**, *14*, 231.
(11) Baker, S.; Robinson, J. S.; Haworth, C. A.; Teng, H.; Smith, R. A.; Chirila, C. C.; Lein, M.; Tisch, J. W. G.; Marangos, J. P. *Science* **2006**, *312*, 424.
(12) Wagner, N. L.; Wuest, A.; Christov, I. P.; Popmintchev, T.; Zhou, X; Murnane, M. M.; Kapteyn, H. C. *Proc. Natl. Acad. Sci.* **2006**, *103*, 13279.

(13) Zhang, G. P. *Phys. Rev. Lett.* **2005**, *95*, 047401.
(14) Averbukh, V.; Alon, O. E.; Moiseyev, N. *Phys. Rev. A* **2001**, *64*, 033411.
(15) (a) Baer, R.; Neuhauser, D.; Zdanska, P. R.; Moiseyev, N. *Phys. Rev. A* **2003**, *68*, 043406. (b) Livshits, E.; Baer, R. *J. Phys. Chem.* **2006**, *110*, 8443.
(16) Gordon, A.; Kartner, F. X; Rohringer, N.; Santra, R. *Phys. Rev. Lett.* **2006**, *96*, 223902.
(17) Onida, G.; Reining, L.; Rubio, A. *Rev. Mod. Phys.* **2002**, *74*, 601.
(18) Burke, K.; Werschnik, J.; Gross, E. K. U. *J. Chem. Phys.* **2005**, *123*, 062206.
(19) Lein, M.; Kreibich, T.; Gross, E. K. U.; Engel, V. *Phys. Rev. A* **2002**, *65*, 033403.
(20) Pronin, K. A.; Bandrauk, A. D. *Phys. Rev. Lett.* **2006**, *97*, 020602.
(21) Suzuki, M.; Mukamel, S. *J. Chem. Phys.* **2003**, *119*, 4722.
(22) (a) Li, X. S.; Tully, J. C.; Schlegel, H. B.; Frisch, M. J. *J. Chem. Phys.* **2005**, *123*, 084106. (b) Li, X. S.; Smith, S. M.; Markevitch, A. N.; Romanov, D. A.; Levis, R. J.; Schlegel, H. B. *Phys. Chem. Chem. Phys.* **2005**, *7*, 233. (c) Isborn, C. M.; Li, X. S.; Tully, J. C. *J. Chem. Phys.* **2007**, *126*, 134307. (d) Schlegel, H. B.; Smith, S. M.; Li, X. S. *J. Chem. Phys.* **2007**, *126*, 244110. (e) Smith, S. M.; Li, X. S.; Markevitch, A.; Romanov, D.; Levis, R. J.; Schlegel, H. B. *J. Phys. Chem. A* **2007**, *111*, 6920.
(23) (a) Chu, S. I. *J. Chem. Phys.* **2005**, *123*, 62207. (b) Chu, S. I.; Telnov, D. A. *Phys. Rep.* **2004**, *390*, 1. (c) Chu, X.; Chu, S.-I. *Phys. Rev. A* **2004**, *70*, 061402. (d) Guan, X. X.; Tong, X. M.; Chu, S. I. *Phys. Rev. A* **2006**, *73*, 23403. (e) Telnov, D. A.; Chu, S. I. *Phys. Rev. A* **2005**, *71*, 13408. (f) Usachenko, V. I.; Chu, S. I. *Phys. Rev. A* **2005**, *71*, 63410.
(24) Sun, J.; Guo, Z. Y.; Liang, W. Z. *Phys. Rev. B* **2007**, *75* 195438.
(25) (a) Bandrauk, A. D.; Ullrich, C. *Time-dependent density functional Theory- New Developments*; Burke, K., Marques, M., Eds.; Springer: New York, 2007. (b) Ullrich1, C. A.; Tokatly, I. V. *Phys. Rev. B* **2006**, *73*, 235102. (c) Kurzweil, Y.; Baer, R. *J. Chem. Phys.* **2004**, *121*, 8731.
(26) Jochnowitz, E. B.; Maier, J. P. *Annu. Rev. Phys. Chem.* **2008**, *59*, 519.
(27) Snow, T. P.; McCall, B. J. *Annu. Rev. Astron. Astrophys.* **2006**, *44*, 367.
(28) Belau, L.; Wheeler, S. E.; Ticknor, B. W.; Ahmed, M.; Leone, S. R.; Allen, W. D.; Schaefer III, H. F.; Duncan, M. A. *J. Am. Chem. Soc.* **2007**, *129*, 10229.
(29) Keldysh, L. V. *Sov. Phys. JETP* **1965**, *20*, 1307.
(30) Sundaram, B.; Milonni, P. W. *Phys. Rev. A* **1990**, *41*, 6571.
(31) Liang, W. Z.; Yokojima, S.; Chen, G. H. *J. Chem. Phys.* **1999**, *110*, 1844.
(32) Sun, J.; Song, J.; Zhao, Y.; Liang, W. Z. *J. Chem. Phys.* **2007**, *127*, 234107.
(33) Shao, Y.; Molnar, L. F.; Jung, Y.; Kussmann, J.; Ochsenfeld, C.; Brown, S. T.; Gilbert, A. T. B.; Slipchenko, L. V.; Levchenko, S. V.; O'Neill, D. P.; DiStasio, R. A.; Lochan, R. C.; Wang, T.; Beran, G. J. O.; Besley, N. A.; Herbert, J. M.; Lin, C. Y.; Van Voorhis, T.; Chien, S. H.; Sodt, A.; Steele, R. P.; Rassolov, V. A.; Maslen, P. E.; Korambath, P. P.; Adamson, R. D.; Austin, B.; Baker, J.; Byrd, E. F. C.; Dachsel, H.; Doerksen, R. J.; Dreuw, A.; Dunietz, B. D.; Dutoi, A. D.; Furlani, T. R.; Gwaltney, S. R.; Heyden, A.; Hirata, S.; Hsu, C. P.; Kedziora, G.; Khalliulin, R. Z.; Klunzinger, P.; Lee, A. M.; Lee, M. S.; Liang, W.; Lotan, I.; Nair, N.; Peters, B.; Proynov, E. I.; Pieniazek, P. A.; Rhee, Y. M.; Ritchie, J.; Rosta, E.; Sherrill, C. D.; Simmonett, A. C.; Subotnik, J. E.; Woodcock, H. L.; Zhang, W.; Bell, A. T.; Chakraborty, A. K.; Chipman, D. M.; Keil, F. J.; Warshel, A.; Hehre, W. J.; Schaefer, H. F.; Kong, J.; Krylov, A. I.; Gill, P. M. W.; Head-Gordon, M. *Phys. Chem. Chem. Phys.* **2006**, *8*, 3172.
(34) Stephens, P. J.; Devlin, F. J.; Chabalowski, C. F.; Frisch, M. J. *J. Phys. Chem.* **1994**, *98*, 11623.
(35) Pacios, L. F.; Christiansen, P. A. *J. Chem. Phys.* **1985**, *82*, 2664.
(36) Nguyen, H. S.; Bandrauk, A. D.; Ullrich, C. A. *Phys. Rev. A* **2004**, *69*, 063415.
(37) Alon, O. E.; Averbukh, V.; Moiseyev, N. *Phys. Rev. Lett.* **1998**, *80*, 3743.
(38) Moiseyev, N.; Lein, M. *J. Phys. Chem. A* **2003**, *107*, 7181.
(39) Bavli, R.; Metiu, H. *Phys. Rev. A* **1993**, *47*, 3299.
(40) (a) Lezuis, M.; Blanchet, V.; Ivanov, M. Yu.; Stolow, A. *J. Chem. Phys.* **2002**, *117*, 1575. (b) Lezuis, M.; Blanchet, V.; Rayner, D. M.; Villeneuve, D. M.; Stolow, A.; Ivanov, M. Yu. *Phys. Rev. Lett.* **2001**, *86*, 51.
(41) Barth, I.; Manz, J.; Shigeta, Y.; Yagi, K. J. *Am. Chem. Soc.* **2006**, *128*, 7043.
(42) Barth, I.; Manz, J. *Angew. Chem., Int. Ed.* **2006**, *45*, 2962.

JP804408A